

MgBr₂ supported on Fe₃O₄@SiO₂ ~ urea nanoparticle: An efficient catalyst for *ortho*-formylation of phenols and oxidation of benzylic alcohols

Ebrahim Soleimani  | Nadieh Yaesoobi | Hamid Reza Ghasempour

Department of Chemistry, Razi University, Kermanshah 67149-67346, Iran

Correspondence

E. Soleimani, Department of Chemistry, Razi University, Kermanshah 67149-67346, Iran.

Email: e_soleimanirazi@yahoo.com

Urea was successfully immobilized on the surface of chloropropyl-modified Fe₃O₄@SiO₂ core-shell magnetic nanoparticles, then supported by MgBr₂ and acts as a unique catalyst for oxidation of benzylic alcohols to aldehydes and ketones, and *ortho*-formylation of phenols to salicylaldehydes. The prepared catalyst was characterized by FT-IR, transmission electron microscopy, scanning electron microscopy, X-ray powder diffraction, dispersive X-ray spectroscopy, CHN and TGA. It was found that Fe₃O₄@SiO₂ ~ urea/MgBr₂ showed higher catalytic activity than homogenous MgBr₂, and could be reused several times without significant loss of activity.

KEYWORDS

alcohol, formylation, magnetite nanocatalyst, MgBr₂, oxidation, salicylaldehyde

1 | INTRODUCTION

In recent years, much attention has been focused on heterogeneous catalysts due to their potential applications for replacing homogenous catalysts in organic chemistry and industry; they exhibit advantages of easy separation of the catalyst from the reaction medium, minimal corrosion, simplified recovery, reusability, green chemical processes and enhanced product selectivity.^[1,2] Among heterogeneous catalysts, supported catalysts on a solid support have attracted significant attention due to a number of advantages, such as their available active sites, stability, and product separation and their recovery, which are all important factors in organic chemistry and industry.^[3,4] Supported catalysts are available on different supports, such as charcoal, alumina, silica and polymers; however, silica displays many advantageous properties, such as excellent stability (chemical as well as thermal), no swelling, high surface area, good accessibility, and in addition organic groups can be robustly anchored to the surface to provide catalytic center.^[5] Recently, magnetic

nanoparticles Fe₃O₄ (MNPs-Fe₃O₄) have attracted additional attention due to their convenient isolation and recovery.^[6] It has been reported that the heterogeneous catalysts supported on MNPs-Fe₃O₄ reveal excellent performance in many reactions, including hydrolysis, hydrogenation, oxidation, carbon-carbon coupling and reduction.^[7]

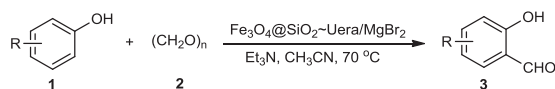
Salicylic aldehydes are excellent precursors for the preparation of important classes of organic compounds, such as coumarins, benzofurans, salen derivatives and industrially useful metal extractants.^[8] Numerous methods are available for preparation of salicylaldehydes; however, formylation of phenols is an important reaction for the synthesis of salicylaldehydes. Moreover, many of the methods involve the use of noxious reagents, harsh reaction conditions, low yields and lack of regioselectivity.^[9] An exception to this is the formylation of phenols using the acceptable reagents MgCl₂, Et₃N and paraformaldehyde, giving high yields of salicylaldehydes from reactions exclusively at the *ortho*-position.^[10]

Magnesium bromide (MgBr_2) is commercially available, inexpensive and generates no toxic byproducts on aqueous work-up, which would allow us to conduct the reactions open to the atmosphere using untreated, reagent-grade solvents. MgBr_2 has found many applications in synthetic organic transformations as a mild Lewis acid in Diels–Alder cycloadditions,^[11] Cannizzaro reactions,^[12] aldol condensation,^[13] α -aminonitrile syntheses,^[14] alcohols protection,^[15] and thiolysis of epoxides^[16] and ring opening of epoxides.^[17]

The use of MgCl_2 or MgBr_2 has received considerable attention as an inexpensive, nontoxic, commercially available catalyst for formylation of phenols. However, in spite of their potential utility, these homogeneous catalysts present limitations due to the use of toxic and corrosive reagents, the tedious work-up procedure, the necessity of neutralization of the strong acid media producing undesired washes, long reactions times and high temperature. Therefore, the discovery of a novel and inexpensive catalyst, which can be easily separated, reused and does not become contaminated by the products, is of prime importance. Therefore, we have prepared a magnetic heterogeneous catalyst of $\text{Fe}_3\text{O}_4@\text{SiO}_2 \sim \text{urea}/\text{MgBr}_2$ by supporting MgBr_2 on $\text{Fe}_3\text{O}_4@\text{SiO}_2 \sim \text{urea}$. To check the applicability of this catalyst, we chose oxidation of benzylic alcohols and *ortho*-formylation of phenols under this new catalyst.

The oxidation of alcohols is one of the most important organic transformation reactions, and studies on the mild oxidation methods of alcohols with less toxic reagents have been carried out extensively. Among these, selective oxidation of benzyl alcohols to benzaldehydes with H_2O_2 on magnetic iron oxides is more appealing because of its many attractive advantages, such as low cost, wide availability, good biocompatibility, high stability and convenient magnetic separation.^[18]

Due to above-mentioned reasons, and as a part of our ongoing research on new nanomagnetic heterogeneous catalysts in the synthesis of organic compounds,^[19] we report herein a mild and efficient approach for the synthesis of salicylaldehydes **3** via *ortho*-formylation of phenols **1** with paraformaldehyde **2** using a catalytic amount of $\text{Fe}_3\text{O}_4@\text{SiO}_2 \sim \text{urea}/\text{MgBr}_2$ and triethylamine in acetonitrile at 70 °C in high yields (Scheme 1).



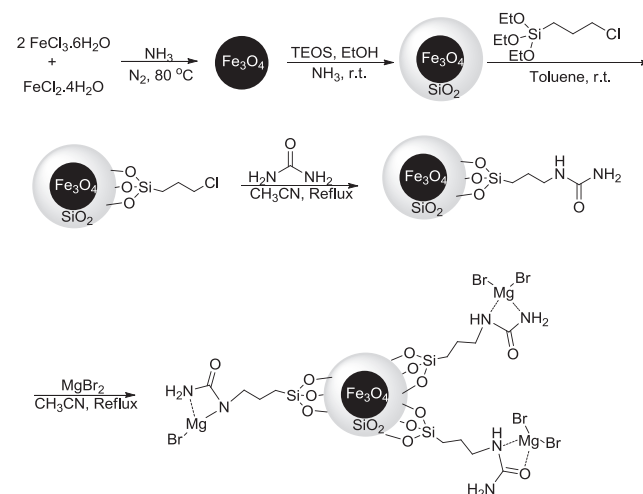
SCHEME 1 Synthesis of salicylaldehydes

2 | RESULTS AND DISCUSSION

2.1 | Preparation and characterization of the catalyst ($\text{Fe}_3\text{O}_4@\text{SiO}_2 \sim \text{urea}/\text{MgBr}_2$)

The $\text{Fe}_3\text{O}_4@\text{SiO}_2 \sim \text{urea}/\text{MgBr}_2$ nanocatalyst was prepared with a four-step reaction; initially by preparing iron oxide as a magnetic core for coating by a silica layer through sol–gel process. For immobilization of the organic catalyst on the surface of inorganic support, the surface was first modified using an appropriate coupling agent to make covalent bonds with the catalyst. It is known that organosilanes can act as a linker between the organic catalyst and the support. In this work, chloropropyltriethoxysilane was used. Scheme 1 illustrates the process of catalyst preparation. A part of the linker's chloride was replaced by nitrogen of the urea via an $\text{S}_{\text{N}}2$ nucleophilic substitution reaction. Then, MgBr_2 was attached onto the surface by interaction between Mg^{2+} and electron paired nitrogens from urea. The catalyst preparation steps are illustrated in Scheme 2. To substantiate this claim, each step of the catalyst preparation procedure was separated and examined by characterization techniques such as FT-IR to ensure the presence of new functional groups. Eventually, the nanocatalyst was studied from different aspects, such as size, size distribution and morphology, and characterized by different techniques, such as X-ray powder diffraction (XRD), transmission electron microscopy (TEM), scanning electron microscopy (SEM), FT-IR, dispersive X-ray spectroscopy (EDX), CHN and TGA.

The crystalline structure of magnetite NPs before and after silica coating was identified using the XRD technique. Figure 1 (see Supporting Information) shows the



SCHEME 2 The schematic pathway for synthesis of $\text{Fe}_3\text{O}_4@\text{SiO}_2 \sim \text{urea}/\text{MgBr}_2$ core–shell NPs

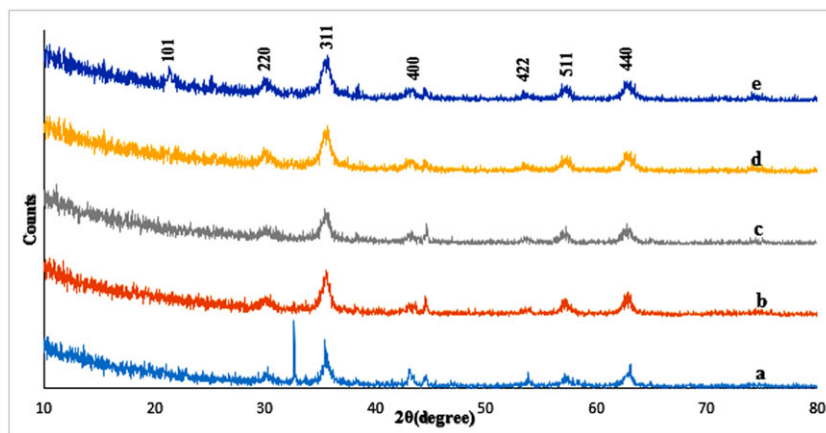


FIGURE 1 XRD patterns of: (a) Fe_3O_4 ; (b) $\text{Fe}_3\text{O}_4@SiO_2$; (c) $\text{Fe}_3\text{O}_4@SiO_2 \sim Cl$; (d) $\text{Fe}_3\text{O}_4@SiO_2 \sim urea$; (e) $\text{Fe}_3\text{O}_4@SiO_2 \sim urea/MgBr_2$. The arrow mark indicates the (101) diffraction peak due to $MgBr_2$

XRD patterns of these samples. The XRD pattern of Fe_3O_4 clearly showed six reflection peaks [2θ at 30° , 36.0° , 43° , 54.0° , 57.5° and 62.5° refer to (220), (311), (400), (422), (511) and (440)] and confirmed the formation of a cubic spinel ferrite structure, and the crystallite size was calculated from the Scherrer's formula and found to be an average diameter of about 20 nm (Figure 1a). Furthermore, no change was observed in the crystalline structure of the Fe_3O_4 core upon coating and immobilization of the magnetite surface by silica (Figure 1b), 3-chloropropyltriethoxysilane (CPTES; Figure 1c), urea (Figure 1d) and $MgBr_2$ (Figure 1e). After immobilization of $MgBr_2$ onto the surface of MNPs, the new diffraction peak appeared at 21.1° and 24.0° attributed to $MgBr_2$.

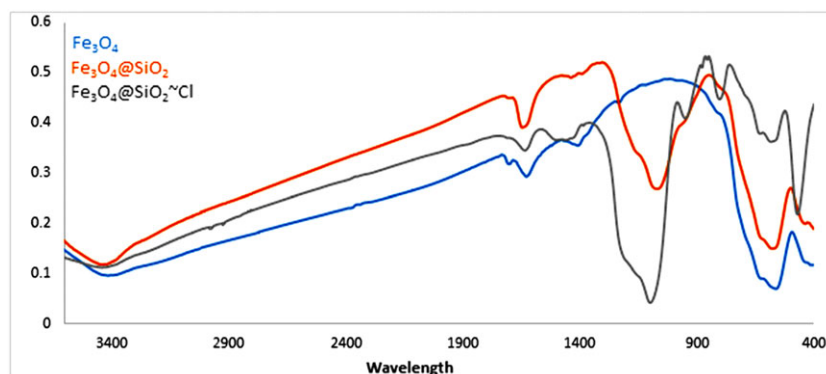
Figures 2 and 3 (also see Supporting Information) show the FT-IR spectra of Fe_3O_4 , $\text{Fe}_3\text{O}_4@SiO_2$, $\text{Fe}_3\text{O}_4@SiO_2 \sim Cl$, $\text{Fe}_3\text{O}_4@SiO_2 \sim urea$ and $\text{Fe}_3\text{O}_4@SiO_2 \sim urea/MgBr_2$. In Figure 2a, the bands at 458 cm^{-1} , 574 cm^{-1} and 620 cm^{-1} are attributed to the vibration of the Fe–O bond, while the band at 3421 cm^{-1} is assigned to the symmetrical stretching vibration of hydroxyl groups (–OHs), indicating the presence of some amount of ferric hydroxide in Fe_3O_4 . The band at 1620 cm^{-1} is attributed to the bending vibration of adsorbed water. Figure 2b shows the FT-IR spectrum of $\text{Fe}_3\text{O}_4@SiO_2$ core-shell MNPs. Comparing Figure 2b with Figure 2a, we found some new absorption peaks in Figure 2b. The bands at 1089 cm^{-1} are related to

the asymmetric stretching vibration and symmetric stretching vibration of Si–O–Si. The band at 960 cm^{-1} is assigned to the symmetric stretching vibration of Si–OH. Figure 2c shows the FT-IR spectrum of $\text{Fe}_3\text{O}_4@SiO_2 \sim Cl$. In Figure 2c, in addition to bands of Fe–O bond, Si–OH and Si–O–Si, newer bands at 2847 cm^{-1} and 2926 cm^{-1} are related to the stretching vibrations of C–H bonds of CPTES, while peaks at 638 cm^{-1} and 689 cm^{-1} are ascribed to the stretching vibrations of C–Cl bonds of CPTES.

The FT-IR spectra of $\text{Fe}_3\text{O}_4@SiO_2 \sim urea$ and $\text{Fe}_3\text{O}_4@SiO_2 \sim urea/MgBr_2$ are shown in Figure 3. The spectra of as-prepared $\text{Fe}_3\text{O}_4@SiO_2 \sim urea$ showed a band due to C = O stretching vibration at 1559 cm^{-1} , N–C–N stretching vibration at 1430 cm^{-1} and N–H stretching vibration at 3410 cm^{-1} . The major peaks of urea overlapped with broad and strong bands of Si–O–Si, intermolecular water and moisture (H–OH, bending) in the samples. Also, this peak appeared in the FT-IR spectrum of $\text{Fe}_3\text{O}_4@SiO_2 \sim urea/MgBr_2$, and showed a new peak due to $MgBr_2$ at 950 cm^{-1} . For confirmation of the functionalization processes and the presence of urea and $MgBr_2$ on the surface, other analyses such as CHN, EDX and TGA analyses were required.

Transmission electron microscopy was used to observe the morphology of the four-stage synthesis of the catalyst. Figure 4a shows that the NPs have a core-shell structure with a distinct contrast between silica shells and Fe_3O_4

FIGURE 2 FT-IR spectra of Fe_3O_4 , $\text{Fe}_3\text{O}_4@SiO_2$ and $\text{Fe}_3\text{O}_4@SiO_2 \sim Cl$



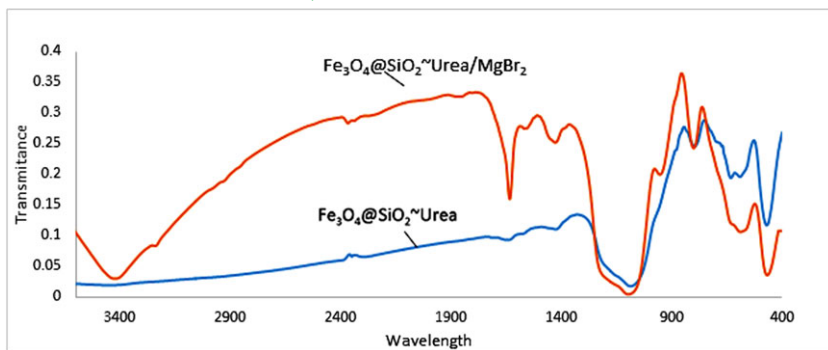


FIGURE 3 FT-IR spectra of $\text{Fe}_3\text{O}_4@SiO_2 \sim \text{urea}$ and $\text{Fe}_3\text{O}_4@SiO_2 \sim \text{urea}/MgBr_2$

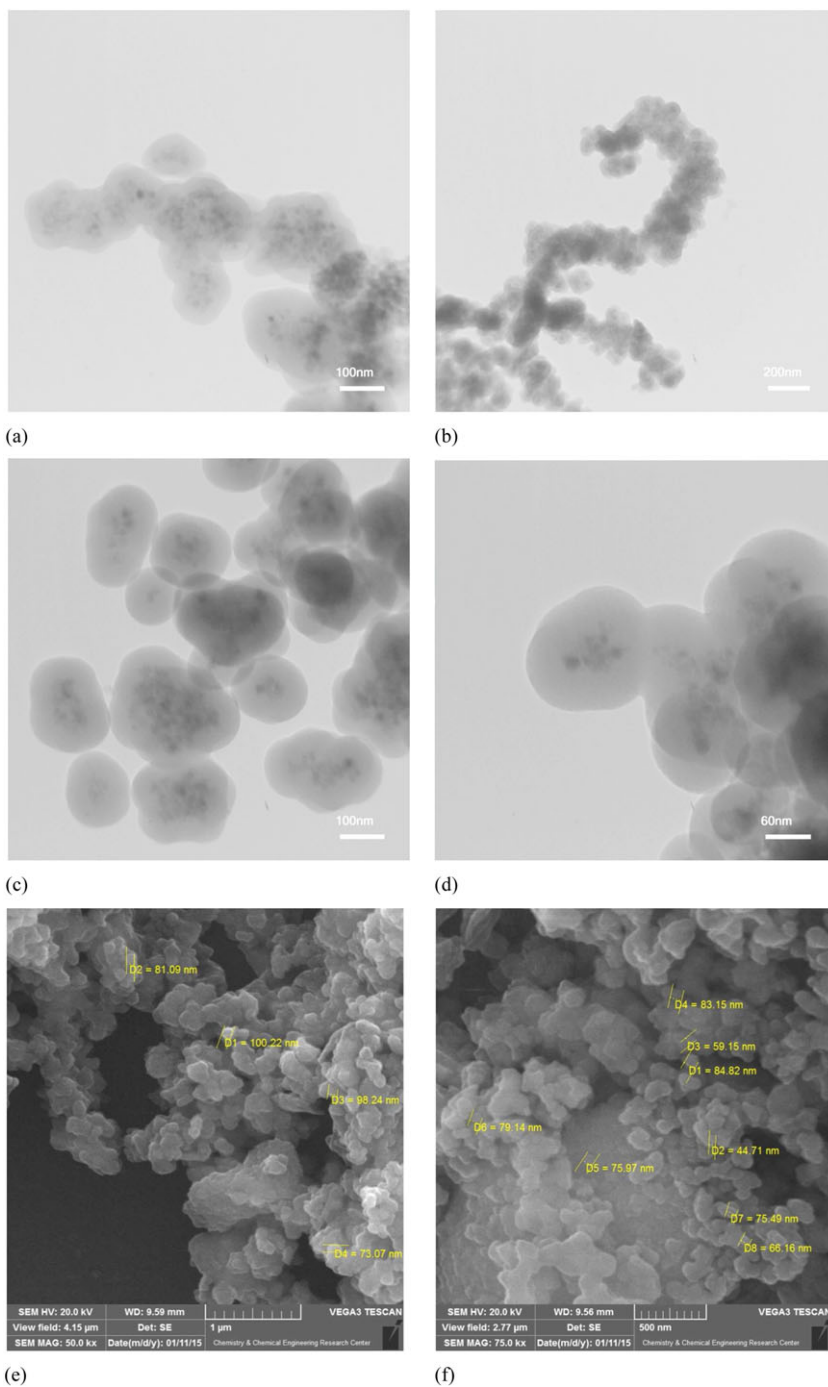


FIGURE 4 TEM images of: (a) $\text{Fe}_3\text{O}_4@SiO_2$; (b) $\text{Fe}_3\text{O}_4@SiO_2 \sim Cl$; (c) $\text{Fe}_3\text{O}_4@SiO_2 \sim \text{urea}$; (d) $\text{Fe}_3\text{O}_4@SiO_2 \sim \text{urea}/MgBr_2$; and SEM images of: (e) $\text{Fe}_3\text{O}_4@SiO_2 \sim \text{urea}$; (f) $\text{Fe}_3\text{O}_4@SiO_2 \sim \text{urea}/MgBr_2$

cores, implying that silica shells ($\text{Fe}_3\text{O}_4@\text{SiO}_2$) successfully coated the hydrophilic Fe_3O_4 NPs. The average size of the cores was found to be $\sim 10\text{--}15$ nm, and the results are consistent with the crystallite size of 12 nm for Fe_3O_4 NPs obtained from the XRD results. The thickness of the silica shell was estimated to be about 20–30 nm. Therefore, the average size of magnetite-silica core-shell NPs was determined to be about 50–80 nm. Similarly, the TEM images of $\text{Fe}_3\text{O}_4@\text{SiO}_2 \sim \text{Cl}$, $\text{Fe}_3\text{O}_4@\text{SiO}_2 \sim \text{urea}$ and $\text{Fe}_3\text{O}_4@\text{SiO}_2 \sim \text{urea}/\text{MgBr}_2$ are shown in Figure 4b–d, respectively. These images reveal that the modified magnetic silica $\text{Fe}_3\text{O}_4@\text{SiO}_2 \sim \text{urea}$ and $\text{Fe}_3\text{O}_4@\text{SiO}_2 \sim \text{urea}/\text{MgBr}_2$ NPs are similar in size ($\sim 55\text{--}85$ nm) and are spherical in shape. The SEM image of $\text{Fe}_3\text{O}_4@\text{SiO}_2 \sim \text{urea}$ and $\text{Fe}_3\text{O}_4@\text{SiO}_2 \sim \text{urea}/\text{MgBr}_2$ in Figure 4e and f shows the granular and spherical morphology for these NPs. The average size of $\sim 44\text{--}100$ nm obtained by SEM analysis is consistent with the TEM results.

Furthermore, the EDX in Figure 5 and Table 1 (see Supporting Information) confirmed the presence of MgBr_2 and urea on surface $\text{Fe}_3\text{O}_4@\text{SiO}_2$.

From the elemental analysis (CHN) in Table 2 (see Supporting Information), it was observed that there was an increase in carbon content, and in hydrogen and nitrogen content after functionalization of the $\text{Fe}_3\text{O}_4@\text{SiO}_2 \sim \text{Cl}$

with urea. This indicated the successful attachment of urea onto the surface of the modified NPs. Also, the elemental analysis of $\text{Fe}_3\text{O}_4@\text{SiO}_2 \sim \text{urea}/\text{MgBr}_2$ showed a decrease in content of these elements because the inorganic content of NPs was increased after immobilization of MgBr_2 on the surface. Therefore, elemental analysis (CHN) of MNPs confirmed the presence of urea and MgBr_2 on the surface.

TGAs of $\text{Fe}_3\text{O}_4@\text{SiO}_2 \sim \text{Cl}$, $\text{Fe}_3\text{O}_4@\text{SiO}_2 \sim \text{urea}$ and $\text{Fe}_3\text{O}_4@\text{SiO}_2 \sim \text{urea}/\text{MgBr}_2$ NPs are presented in Figure 6 (see Supporting Information). The initial wt% losses below 150 °C are related to the adsorbed moisture in the samples. The decomposition temperature, which started at 460 °C, and continued until 530 °C, is associated with the decomposition of the organic chains. The organic species decomposed completely at temperatures higher than 600 °C, and the residual weights of $\text{Fe}_3\text{O}_4@\text{SiO}_2 \sim \text{Cl}$, $\text{Fe}_3\text{O}_4@\text{SiO}_2 \sim \text{urea}$ and $\text{Fe}_3\text{O}_4@\text{SiO}_2 \sim \text{urea}/\text{MgBr}_2$ were 90%, 86% and 91%, respectively, at 700 °C. In other words, the results demonstrate percentages of 10%, 4% and 9% for organic groups on the surface of $\text{Fe}_3\text{O}_4@\text{SiO}_2 \sim \text{Cl}$, $\text{Fe}_3\text{O}_4@\text{SiO}_2 \sim \text{urea}$ and $\text{Fe}_3\text{O}_4@\text{SiO}_2 \sim \text{urea}/\text{MgBr}_2$, respectively. The $\text{Fe}_3\text{O}_4@\text{SiO}_2 \sim \text{urea}/\text{MgBr}_2$ NPs showed a lower percentage of organic groups on the surface due to the presence of MgBr_2 on the surface.

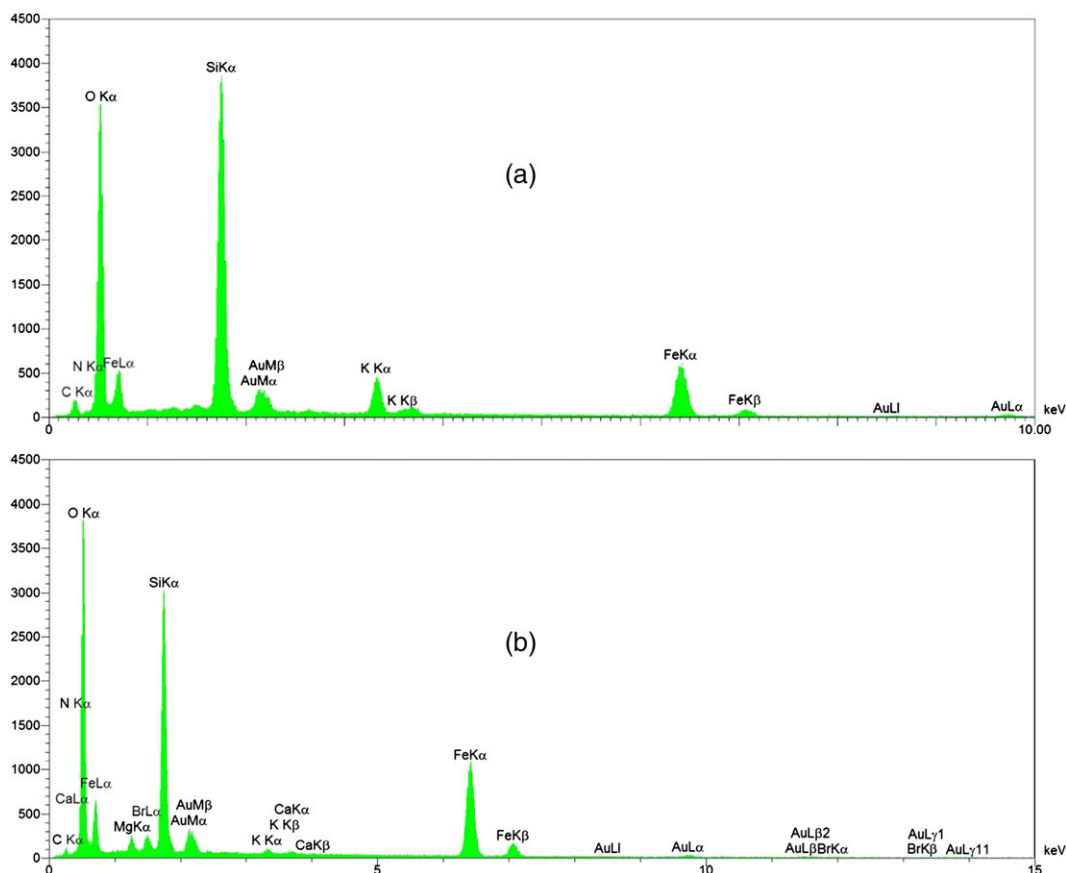


FIGURE 5 EDX spectra of: (a) $\text{Fe}_3\text{O}_4@\text{SiO}_2 \sim \text{urea}$; and (b) $\text{Fe}_3\text{O}_4@\text{SiO}_2 \sim \text{urea}/\text{MgBr}_2$

TABLE 1 EDX data of $\text{Fe}_3\text{O}_4@\text{SiO}_2 \sim \text{urea}$ and $\text{Fe}_3\text{O}_4@\text{SiO}_2 \sim \text{urea}/\text{MgBr}_2$ (wt%)

Element (wt%)	$\text{Fe}_3\text{O}_4@\text{SiO}_2 \sim \text{urea}$	$\text{Fe}_3\text{O}_4@\text{SiO}_2 \sim \text{urea}/\text{MgBr}_2$
C	2.97	1.54
N	0.75	0.57
O	17.35	14.77
Mg	–	4.55
Si	15.59	11.79
Fe	63.35	60.69
Br	–	6.19
Total	100.00	100.00

TABLE 2 The elemental analysis (CHN) results

Elements (mg g ⁻¹)	Fe/ SiO ₂ ~ Cl	Fe/ SiO ₂ ~ urea	Fe/SiO ₂ ~ urea/ MgBr ₂
N	0	5.714	2.012
C	30.232	37.623	23.914
H	2.071	4.430	1.584

2.2 | Catalytic activity of $\text{Fe}_3\text{O}_4@\text{SiO}_2 \sim \text{urea}/\text{MgBr}_2$ MNPs in the synthesis of salicylaldehydes

We chose the reaction of phenol and paraformaldehyde as a model system for the optimization study (Table 3). First, we compared the reaction rate in different solvents, such as water, dichloromethane, toluene and acetonitrile, by measuring the isolated yield using identical amounts of $\text{Fe}_3\text{O}_4@\text{SiO}_2 \sim \text{urea}/\text{MgBr}_2$ for a fixed reaction time of 24 h at room temperature (entries 1–4). The desired product was obtained in acetonitrile and toluene (entries 3 and 4), but the best result was obtained when acetonitrile was utilized. Next, we studied the model reaction at different

temperatures using identical amounts of $\text{Fe}_3\text{O}_4@\text{SiO}_2 \sim \text{urea}/\text{MgBr}_2$ for a fixed reaction time of 1 h in acetonitrile (entries 4–7). The reaction rate increased as the temperature was raised. At 70 °C, the maximum yield (97%) was obtained in a reaction time of 1 h (entry 6). The model reaction in acetonitrile at 70 °C was also studied using different amounts of $\text{Fe}_3\text{O}_4@\text{SiO}_2 \sim \text{urea}/\text{MgBr}_2$ (entries 6, 8, 9). The best results were obtained with 0.05 g of $\text{Fe}_3\text{O}_4@\text{SiO}_2 \sim \text{urea}/\text{MgBr}_2$ (entry 6). Also, when the reaction was under solvent-free conditions, the reaction yield was only 51% after 12 h (entry 10). Further work indicated that the best results were obtained when the reaction was carried out at 70 °C for 1 h in acetonitrile using 0.05 g of $\text{Fe}_3\text{O}_4@\text{SiO}_2 \sim \text{urea}/\text{MgBr}_2$ (entry 6).

With the optimized condition established above, we next attempted to extend various types of phenols; the results are summarized in Table 4. In all cases, excellent yields were obtained.

The recyclability and reusability of the catalyst was studied by using a model reaction. This heterogeneous catalyst can be easily recovered with an external magnet and reused for at least five cycles without a significant decrease in the catalytic activity and performance (Figure 7; see Supporting Information).

To show the efficiency of $\text{Fe}_3\text{O}_4@\text{SiO}_2 \sim \text{urea}/\text{MgBr}_2$ in comparison with other reported catalysts, we summarized some of the results for the synthesis of coumarins obtained by other workers. It is clear from Table 5v that the current method is simpler, more efficient and less time consuming for the synthesis of coumarin derivatives. In addition, in this method, this heterogeneous catalyst ($\text{Fe}_3\text{O}_4@\text{SiO}_2 \sim \text{urea}/\text{MgBr}_2$) was recovered easily and was reused without a significant decrease in the catalytic activity.

Finally, for further exploration of the scope and limitation of the method, we investigated the oxidation of different benzylic alcohols with this new catalyst in the presence of hydrogen peroxide. Gratifyingly the reaction

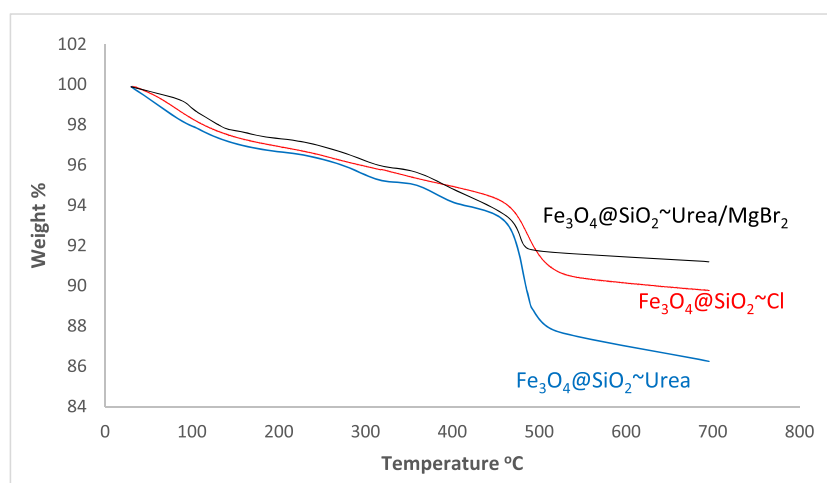
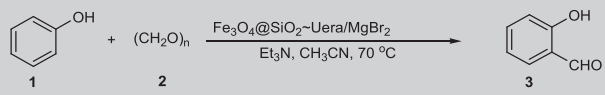
**FIGURE 6** TGA curves of $\text{Fe}_3\text{O}_4@\text{SiO}_2 \sim \text{Cl}$, $\text{Fe}_3\text{O}_4@\text{SiO}_2 \sim \text{urea}$ and $\text{Fe}_3\text{O}_4@\text{SiO}_2 \sim \text{urea}/\text{MgBr}_2$

TABLE 3 Optimization of reaction conditions for synthesis of salicylaldehyde^a


Entry	Fe ₃ O ₄ @SiO ₂ ~ urea/MgBr ₂ (g)	Solvent	Temperature (°C)	Time (h)	Yield% ^b
1	0.05	H ₂ O	r.t.	12	Trace
2	0.05	Dichloromethane	r.t.	12	Trace
3	0.05	Toluene	r.t.	24	23
4	0.05	Acetonitrile	r.t.	24	38
5	0.05	Acetonitrile	50	1	60
6	0.05	Acetonitrile	70	1	97
7	0.05	Acetonitrile	80	1	97
8	0.07	Acetonitrile	70	1	97
9	0.03	Acetonitrile	70	1	83
10	0.05	Solvent-free	80	12	51

^aReaction conditions: phenol (1.0 mmol), paraformaldehyde (4 mmol) and triethylamine (1.5 mmol).

^bIsolated yields.

led to the formation of the corresponding aromatic aldehydes or ketones in high isolated yields (Table 6).

2.3 | Proposed mechanism

A possible mechanism for salicylaldehyde derivatives by MgCl₂ has been proposed previously.^[21] Scheme 3 shows a possible mechanism for this synthesis in the presence of Fe₃O₄@SiO₂ ~ urea/MgBr₂. We expected the mechanism by Fe₃O₄@SiO₂ ~ urea/MgBr₂ and MgCl₂ to be the same.

3 | EXPERIMENTAL

3.1 | Preparation of modified silica-coated magnetite NPs (Fe₃O₄@SiO₂ ~ Cl)

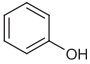
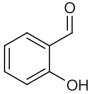
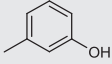
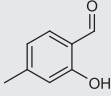
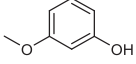
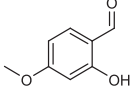
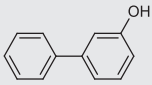
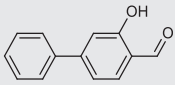
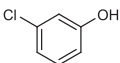
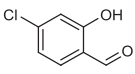
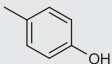
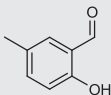
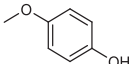
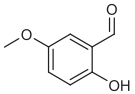
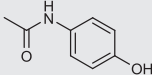
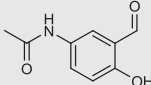
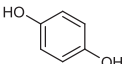
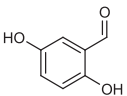
Magnetite (Fe₃O₄) NPs were prepared according to the reported method (co-precipitation),^[24] and coated with silica by tetraethyl orthosilicate (TEOS) in the presence of 2-propanol (sol-gel method).^[25] In brief, 0.036 mol of FeCl₃H₂O and 0.018 mol of FeCl₂4H₂O were dissolved in 20 ml deionized water under nitrogen gas with vigorous stirring. Then, NH₃ (25%) was added into the solution until the pH of the solution reached 11. Stirring was continued for 1 h at 60 °C. The color of the bulk solution turned from orange to black immediately. The magnetite precipitate was separated from the solution using a magnet, washed several times with deionized water and ethanol, and left to dry in air. Then, 0.3 g as-synthesized Fe₃O₄ NPs were mixed with 100 ml isopropyl alcohol in a sealed

three-neck flask by ultrasonic treatment for 30 min. Then, 50 ml deionized water, 3.0 ml TEOS (silica precursor) and 17.0 ml ammonia (25 wt%) were added into the mixture at 30 °C under mechanical agitation. After 12 h, the final product (Fe₃O₄@SiO₂) was collected, washed with ethanol and deionized water, and dried at 50 °C. The silica-coated Fe₃O₄ (Fe₃O₄@SiO₂) NPs were then functionalized using a post-modification method with CPTES^[26] by refluxing in anhydrous toluene at 110 °C for 24 h (Fe₃O₄@SiO₂ ~ Cl). In brief, 2 g of as-synthesized Fe₃O₄@SiO₂ NPs was dispersed in 25 ml of CPTES solution [4%, v/v in dry toluene (99%)]. The mixture was stirred for 24 h under a reflux at 110 °C. After cooling, the sample was collected from the solution using an external magnet, and washed thoroughly twice with ethanol and once with distilled water to remove unreacted CPTES. The solid residue was dried under vacuum conditions at 100 °C for 24 h.

3.2 | Immobilization of urea on the surface of modified silica-coated magnetite NPs (Fe₃O₄@SiO₂ ~ urea)

Urea (0.6 g, 10 mmol) was added into a suspension of Fe₃O₄@SiO₂ ~ Cl (1.0 g), KI (0.16 g, 1 mmol) and K₂CO₃ (0.14 g, 1 mmol) in acetonitrile (30 ml). The reaction mixture was refluxed at 80 °C in an oil bath for 24 h. The solid phase was filtered by applying an external magnet and washed with acetonitrile, followed by distilled water. Finally, the solid sample was dried at 100 °C for 24 h.

TABLE 4 Synthesis of salicylaldehyde derivatives by catalyst $\text{Fe}_3\text{O}_4@\text{SiO}_2 \sim \text{urea}/\text{MgBr}_2^{\text{a}}$

Entry	Substrate	Product	Time (h)	Yield (%) ^b
1			1	97
2			1.5	91
3			1	89
4			2.5	90
5			2	94
6			1	92
7			1	74
8			1	80
9			1	96

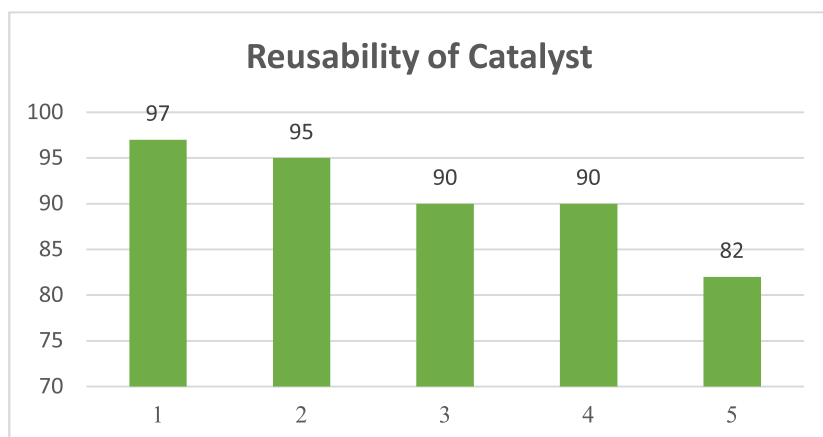
^aReaction condition: phenol (1.0 mmol) and paraformaldehyde (4 mmol) and triethylamine (1.5 mmol).^bIsolated yields.**FIGURE 7** Reusability of the catalyst for synthesis of salicylaldehydes (model reaction: entry 1, Table 4)

TABLE 5 Comparison of the efficiencies of various catalysts used in ortho-formylation of phenols to salicylaldehydes

Catalyst	Condition	Time (h)	Yield (%)	Reference
Montmorillonite KSF	Toluene 100 °C,	4	65–70	[20]
MgCl ₂	Acetonitrile, reflux	1.5–44	5–99	[21]
SnCl ₄	Toluene 100 °C, under an argon atmosphere	8	37–62	[22]
CH ₃ CH ₂ MgBr	Toluene 90 °C, HMPA	3	Up to 40	[23]
Fe ₃ O ₄ @SiO ₂ ~ urea/MgBr ₂	Acetonitrile, 90 °C	1–2.5	74–97	This work

3.3 | Anchoring the magnesium bromide onto the Fe₃O₄@SiO₂ ~ urea (Fe₃O₄@SiO₂ ~ urea/MgBr₂)

A quantity of 1 g of as-synthesized Fe₃O₄@SiO₂ ~ urea NPs was dispersed in 10 ml of acetone solution containing 0.19 g of magnesium bromide. The reaction mixture was stirred for 12 h at room temperature. The solid phase was filtered by applying an external magnet and washed twice with deionized water. Then, the solid sample was dried at 100 °C for 12 h.

3.4 | Oxidation of benzylic alcohols to aldehydes or ketones in the presence of Fe₃O₄@SiO₂ ~ urea/MgBr₂ as a recyclable catalyst

To a solution of benzylic alcohol (1.0 mmol) in aqueous hydrogen peroxide (3 ml, 30%) was added Fe₃O₄@SiO₂ ~ urea/MgBr₂ nanocatalyst (0.02 g) and the reaction mixture was stirred at 60 °C. After 2 h, the nanocatalyst was separated from the reaction mixture by applying an external magnet, and further washed with ethanol and reused in subsequent reactions five times without any loss of activity. Then, the organic layer was separated and the aqueous layer was extracted with ethylacetate (2 × 3 ml). The combined ethylacetate layer was washed with saturated brine (2 × 5 ml) and dried with anhydrous MgSO₄. After evaporation of the solvent, the residue was purified by column chromatography (SiO₂, hexane–EtOAc = 3:1) to afford pure carbonyl compound. All products are known compounds, which were characterized by FT-IR and spectral data, and their mp values were compared with literature reports.

3.5 | Synthesis of salicylaldehyde in the presence of Fe₃O₄@SiO₂ ~ urea/MgBr₂ as a recyclable catalyst

A solution of the selected phenol (1 mmol), paraformaldehyde (4 mmol, 0.12 g), triethylamine (1 mmol, 0.14

ml) and the Fe₃O₄@SiO₂ ~ urea/MgBr₂ nanocatalyst (0.05 g) in acetonitrile (5 ml) was heated at 70 °C in a round-bottom flask in N₂ atmosphere under efficient stirring. After 1 h, the nanocatalyst was separated from the reaction mixture by applying an external magnet, and further washed with ethanol and reused in subsequent reactions five times without any loss of activity. Then, the solvents were evaporated and the crude was purified by recrystallization over acetone. All products are known compounds, which were characterized by FT-IR and spectral data, and their mp values were compared with literature reports.

3.6 | Characterization techniques

Infrared spectra were recorded using a Ray Leigh Wqf-510 FT-IR spectrophotometer. Morphological study measurements were performed using a TEM (Philips CM10) operated at an 80 kV electron beam accelerating voltage. SEM and EDX were performed on a Philips XL-300 instrument. The sample was sputtered by gold to avoid undesirable electron charging. XRD was conducted using a Philips X'pert Pro (PW 3040) X-ray diffractometer with monochromatic Cu-Kα radiation (k_{1/4} 1.54056 °Å, 40 kV, 30 mA). TGAs were investigated using a TG/DTA6300 instrument, at a heating rate of 20 °C min⁻¹ under nitrogen flow. Elemental analysis was performed with a CHN machine (Perkin Elmer Series II, 2400). ¹H and ¹³C NMR spectra were recorded on a Bruker DRX-400 spectrometer at 400 and 100 MHz, respectively. All of the chemicals were purchased from Fluka, Merck and Aldrich, and used without further purification.

4 | CONCLUSION

This work reported on the preparation of Fe₃O₄@SiO₂ ~ urea/MgBr₂ via functionalization of silica-coated magnetic NPs with CPTES as a linker for the immobilization of urea and then incorporation of MgBr₂ on the surface of urea by an electron interaction between Mg²⁺

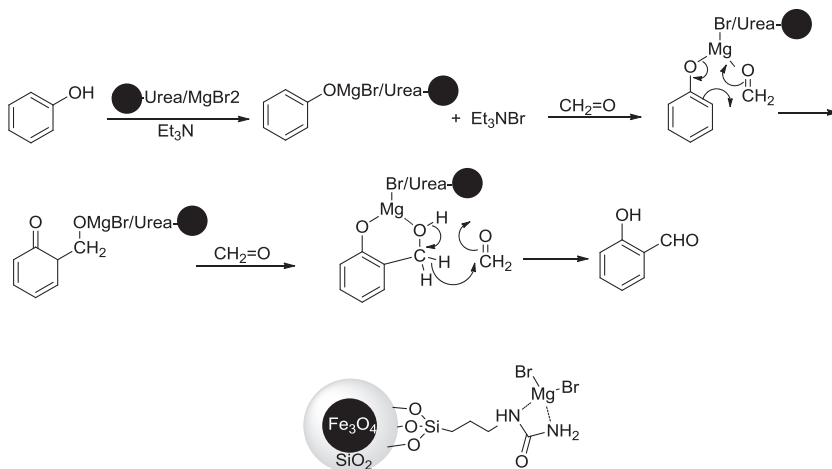
TABLE 6 Selective oxidation of benzylic alcohol to aromatic aldehyde or ketone^a

Entry	Substrate	Product	Time (h)	Yield (%) ^b
1			2	97
2			1.5	98
3			1.5	93
4			2	92
5			2	93
6			2	85
7			2	91
8			2	94
9			2	93
10			1.5	92
11			1.5	93

^aReaction condition: Benzylic alcohol (1.0 mmol), H₂O₂ (3 mL), Fe₃O₄@SiO₂-Urea/MgBr₂ (0.05 g) in acetonitrile solvent.^bIsolated yields.

and N or NH of urea. The core-shell NPs were stable and reusable, and the non-toxic and inexpensive

heterogeneous nanocatalyst prepared has great potential for applications in organic syntheses. The



SCHEME 3 Proposed mechanism for synthesis of salicylaldehydes by $\text{Fe}_3\text{O}_4@\text{SiO}_2 \sim \text{urea}/\text{MgBr}_2$

$\text{Fe}_3\text{O}_4@\text{SiO}_2 \sim \text{urea}/\text{MgBr}_2$ NPs were developed as a catalyst for oxidation of benzylic alcohols to aromatic aldehydes and ketones, and *ortho*-formylation of phenols to salicylaldehydes. The magnetically recoverable catalyst was found to be capable of repeated reuse without significant loss of activity.

ACKNOWLEDGEMENTS

The authors gratefully acknowledge financial support from the Iran National Science Foundation (INSF) and the Research Council of Razi University.

ORCID

Ebrahim Soleimani  <http://orcid.org/0000-0002-5188-8527>

REFERENCES

- [1] E. Nikolla, Y. Roman-Leshkov, M. Moliner, M. E. Davis, *ACS Catal.* **2011**, *1*, 408.
- [2] P. Barbaro, F. Liguori, *Chem. Rev.* **2009**, *109*, 515.
- [3] D. C. Sherrington, A. P. Kybett, *Supported Catalysts and Their Applications*, RSC, Cambridge, UK **2001**.
- [4] P. Munnik, P. E. de Jongh, K. P. de Jong, *Chem. Rev.* **2015**, *115*, 6687.
- [5] (a) C. K. Bradsher, R. D. Brandau, J. E. Boliek, T. L. Hough, *J. Org. Chem.* **1969**, *34*, 2129. (b) A. E. Legrand, *The Surface Properties of Silicas*, Wiley, Chichester **1998**. (c) K. D. Kim, S. S. Kim, Y. H. Choa, H. T. Kim, *J. Ind. Eng. Chem.* **2007**, *13*, 1137. (d) M. Jafarzadeh, R. Adnan, M. K. N. Mazlan, *J. Non-Cryst. Solids* **2012**, *385*, 2981.
- [6] (a) J. Wang, B. Xu, H. Sun, G. Song, *Tetrahedron Lett.* **2013**, *54*, 238. (b) S. D. Pan, H. Y. Shen, L. X. Zhou, X. H. Chen, Y. G. Zhao, M. Q. Cai, M. C. Jin, *J. Mater. Chem. A* **2014**, *2*, 15 345. (c) B. Guoyi, L. Xingwang, L. Xiaofang, *Green Chem.* **2014**, *16*, 3160.
- [7] (a) V. Polshettiwar, R. Luque, A. Fihri, H. Zhu, *Chem. Rev.* **2011**, *111*, 3036. (b) B. Dam, S. Nandi, A. K. Pal, *Tetrahedron Lett.* **2014**, *55*, 5236.
- [8] (a) V. Lehnert, *Tetrahedron* **1972**, *28*, 663. (b) P. Nore, E. J. Honkanen, *Heterocyclic Chem* **1980**, *B*, 985. (c) J. F. Larrow, S. E. Schaus, E. N. Jacobsen, *J. Am. Chem. Soc.* **1996**, *118*, 7420. (d) R. W. Quan, Z. Li, E. N. Jacobsen, *J. Am. Chem. Soc.* **1996**, *118*, 8156.
- [9] (a) G. A. Olah, L. Ohannasian, M. Arvanaghi, *Chem. Rev.* **1987**, *87*, 671. (b) H. Gilman, R. L. Bebb, *J. Am. Chem. Soc.* **1939**, *61*, 109. (c) T. Laird, in *Comprehensive Organic Chemistry*, (Ed: J. F. Stoddart) Vol. 1, Pergamon, Oxford **1979** 1105.
- [10] (a) T. V. Hansen, L. Skattebøl, *Org. Synth.* **2005**, *82*, 64. (b) Ø. W. Akselsen, L. Skattebøl, T. V. Hansen, *Tetrahedron Lett.* **2009**, *50*, 6339.
- [11] D. E. Ward, M. S. Abaee, *Org. Lett.* **2000**, *2*, 3937.
- [12] M. S. Abaee, R. Sharifi, M. M. Mojtahedi, *Org. Lett.* **2005**, *7*, 5893.
- [13] M. S. Abaee, M. M. Mojtahedi, M. M. Zahedi, R. Sharifi, *Heteroatom Chem.* **2007**, *18*, 44.
- [14] M. M. Mojtahedi, M. S. Abaee, H. Abbasi, *Can. J. Chem.* **2006**, *429*.
- [15] M. M. Mojtahedi, H. Abbasi, M. S. Abaee, *J. Mol. Catal. A: Chem.* **2006**, *250*, 6.
- [16] M. M. Mojtahedi, M. S. Abaee, M. Bolourtchian, H. Abbasi, *Phosphorus, Sulfur Silicon Relat. Elem.* **2007**, *182*, 905.
- [17] (a) P. Lupattelli, C. Bonini, L. Caruso, A. Gambacorta, *J. Org. Chem.* **2003**, *68*, 3360. (b) G. Righi, G. Rumboldt, *J. Org. Chem.* **1996**, *61*, 3557.
- [18] (a) S. Xiao, C. Zhang, R. Chen, F. Chen, *New J. Chem.* **2015**, *39*, 4924. (b) F. Chen, S. Xie, X. Huang, X. Qiu, *J. Hazard. Mater.* **2017**, *322*, 152. (c) L. Xiong, R. Chen, F. Chen, *RSC Adv.* **2016**, *6*, 101 048.
- [19] (a) M. Jafarzadeh, E. Soleimani, P. Norouzi, R. Adnan, H. Sepahvand, *J. Fluorine Chem.* **2015**, *178*, 219. (b) M. Jafarzadeh, E. Soleimani, H. Sepahvand, R. Adnan, *RSC Adv.* **2015**, *5*, 42 744. (c) E. Soleimani, M. Jafarzadeh, P. Norouzi, J. Dayou, C. S. Sipaut, R. F. Mansa, P. Saei, *J. Chin. Chem. Soc.* **2015**, *62*, 1155. (d) E. Soleimani, M. Naderi, H.

- Sepahvand, *Appl. Organomet. Chem.* **2016**, <https://doi.org/10.1002/aoc.3566>.
- [20] F. Bigi, M. L. Conforti, R. Maggi, G. Sartori, *Tetrahedron* **2000**, *56*, 2709.
- [21] N. U. Hofsløkken, L. Skattebol, *Acta Chem. Scand.* **1999**, *53*, 258.
- [22] G. Casiraghi, G. Casnati, G. Puglia, G. Sartori, G. Terenghi, *J. Chem. Soc. Perkin Trans.* **1862**, *1*, 1980.
- [23] J. L. Wang, K. Aston, D. Limburg, C. Ludwig, A. E. Hallinan, F. Koszyk, B. Hamper, D. Brown, M. Graneto, J. Talley, T. Maziasz, J. Masferrer, J. Carter, *Bioorg. Med. Chem. Lett.* **2010**, *20*, 7164.
- [24] L. Chen, Z. Xu, H. Dai, S. Zhang, *J. Alloys Compd.* **2010**, *497*, 221.
- [25] W. Stober, A. Fink, E. Bohm, *J. Colloid Interface Sci.* **1968**, *26*, 62.
- [26] F. Adam, H. Osman, K. M. Hello, *J. Colloid Interface Sci.* **2009**, *331*, 143.

How to cite this article: Soleimani E, Yaesoobi N, Ghasempour HR. MgBr₂ supported on Fe₃O₄@SiO₂ ~ urea nanoparticle: An efficient catalyst for *ortho*-formylation of phenols and oxidation of benzylic alcohols. *Appl Organometal Chem.* 2017;e4006. <https://doi.org/10.1002/aoc.4006>